The Journal of Engine Research, Vol. 57 (Winter 2020), pp. 51-64

The Journal of Engine Research

Journal Homepage: www.engineresearch.ir

Air-fuel Mixture Preparation for Internal Combustion Engines: Optical Techniques for Diagnosis of the Spray Developments

L. Allocca[1*], A. Montanaro[2]

[1] *sr. Researcher, Istituto Motori – CNR, Italy,* *l.allocca@im.cnr.it*
[2] *Researcher, Istituto Motori – CNR, Italy,* *a.montanaro@im.cnr.it*
**Corresponding Author*

ARTICLE INFO

Article history:
Received: 7 November 2019
Accepted: 18 February 2020

Keywords:
IC Engine
Combustion
Optical diagnosis
gasoline direct injection
liquid/vapor fuel

ABSTRACT

Nobody escapes the importance of the air/fuel mixture preparation in internal combustion engines, whatever is the thermodynamic cycle they work on and the adopted fuel. The short time between the fueling and the start of the combustion is crucial for the best mixture formation and its burning for energy optimization and the pollutant production. The always stringent vehicle emissions rules led engine research toward the use of high-pressures and direct-injection systems for allowing a best atomization/vaporization of the fuel while, as drawback, the downsizing of the combustion system results in increasing of fuel impact on the combustion chamber and cylinder line with HC and particulate matter increase at the exhaust. A complete description of the injected fuel, its spread in the chamber with primary and secondary breakups, the vaporization, the mixture with the air and the combustion are of basic importance to govern the process and help new design architectures. Optical characterization has shown it's powerful in describing these processes without interfering with their evolution both in stationary and reciprocating devices. Imaging and spectroscopic techniques allow us to follow the physic-chemical transformations of the initial bulk of fuel in the mixture, production of primary and secondary species and individuate the potential sites of pollutant production. Furthermore, the results constitute a data set for initializing and calibrating numerical codes for provisional, results and behavior of diverse injecting systems and at different ambient conditions, and last but not the least inside the engine. In this paper, a tracking shot of optical techniques adopted to depict the fuel spread in a quiescent optical accessible vessel at engine-like conditions is reported for practices of fuel direct injection in engines.

1) Introduction

In the last years, engine technology has been substantially improved by developments of electronic control, increased injection pressure, innovative injection technology, and improved charging technology. The injection system of direct injection (DI) for both diesel and spark-assisted engines has an important role regarding the fulfillment of demands for low pollutant emissions and high engine efficiency. One of the injection system parameters for diesel engines affecting fuel spray characteristics, fuel-air mixing and consequently, combustion and pollutant formation is the geometry of the nozzle hole influencing the liquid spread in the combustion chamber [1, 2].
The fuel atomization and vaporization during the injection phase influence the combustion process significantly so, as a result, an extensive amount of investigation work needs to be performed in the field of the spray characterization. Likewise, the direct injection has growth significantly in the last years for spark-assisted engines with the adoption of the so-called Gasoline Direct Injection (GDI) that, coupled with a massive use of the electronic technology, gives a greatest control of the in-cylinder air-to-fuel ratio with the possibility to operate at higher compression ratios concerning Port Fuel Injection (PFI) ones.
Hence, it is possible to achieve different characteristics for the charge depending on the specific load or speed, as the homogeneous model for stoichiometric or stratified mixtures for lean overall operations. Since the liquid is directly injected into the combustion chamber, the fuel spray characteristics strongly influence the process of fuel-air mixing and combustion [3, 4].
Rapid atomization and vaporization of the fluid are highly desirable. The idea to stimulate the generation of a low penetrating and fast vaporizing fuel spray has driven the research toward the possibility to promote the thermodynamic break-up of the liquid jet during the injection. A further key factor for better atomization is the injection pressure. Higher injection pressures facilitate better fuel atomization and vaporization but, at the same time, creates an over-penetrating factor, so optimization is required [5].
The always shorter distance between the injector nozzle and the piston head/cylinder walls due to the engine downsizing requirements, the major drawbacks of the GDI system produces in a strong impingement of liquid fuel on the combustion chamber wall with highest HC emissions and soot formation due to the fuel cooling and delayed vaporization [6, 7].
The basic spray investigation is the experimental one, typically adopting non-intrusive tools based on optic systems and is carried out on facilities reproducing engine ambient conditions. A different method consists in evaluating mathematically the phenomena occurring in the spray formation process and their influences on the combustion using multidimensional computational fluid dynamic (CFD) codes. The analytical approach, once validated with experimental results, permits to realize an easy and wide variety of operative engine conditions that would be impossible or extremely expensive on physical plants.
A huge amount of detailed experimental data is produced with complex set-ups, making use of innovative techniques, while the numerical work calibrates and tests improved models permitting a quite fast and cheap investigation on complex and multi-variable devices like engines are. Worldwide circuits, like the Engine Combustion Network (ECN), are dedicated to experimental and modeling collaborations on the engine and publishing an internet data archive library where quantitative comparison of spray experiments at engine conditions are available with sprays evaporating and mixing at high-pressure, high-temperature conditions in quiescent vessels [8-10].
This work aims to report an overview of the techniques used for measuring the fuel injection rates and for characterizing the sprays evolutions at the different conditions for the various fuels, injected at high pressures and for variegated back conditions in the optically-accessible vessel. Different settings were realized for the diesel and the gasoline liquids to comply with their engine thermodynamic ambient with non-vaporizing/vaporizing conditions while free-evolving sprays such as impacting ones on heated surfaces were realized. Mie-scattering technique was considered for describing the liquid part of the fuel while shadowgraph/schlieren ones, sensible to the gradient densities of the samples were used for the vapor phases in cycle-resolved sequences of injections. Finally, a customized auto-adaptive software was built up to process the images, distinguishing from the background and noises (mainly generated from the convective motion inside the vessel) permitting to extract the parameters of interest.

2) Experimental apparatus

The experimental characterization of the injection process was carried out under evaporative and non-evaporative conditions injecting the fuel in a high-pressure constant-volume vessel to measure the spatial and temporal evolution of the spray pattern for different engine-like gas densities.
Figure 1 shows a photo of the test chamber in the experimental setup context. Three orthogonal 80 mm in diameter quartz windows permit the access to the investigated area, a fourth one is for housing the injector holder. The vessel was kept at ambient temperature in nitrogen gas at atmospheric backpressure and there was no combustion during the tests while a vacuum pump realized the sub-atmospheric experimental conditions down to 0.03 MPa. A pneumatic high-pressure injection system pressurized the fluid up to 300 MPa and fed the fluid to the injector. No rotating organs were on the apparatus and an external TTL signals draw the injector. This is located on the top of the vessel in a holder including a jacket connected to a chiller for fluxing the liquid fixing the temperature. The fuel is in a heated tank and its temperature is measured by a J-type thermocouple located close to the pipe-injector connection.

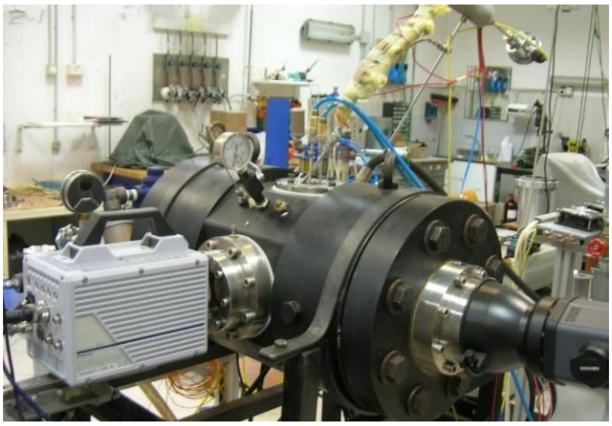

Figure 1: Photo of the optical high-pressure test chamber

Figure 2 reports a schematic of the nozzle (T_i) and the fuel (T_f) temperature governor; a homemade software controls and manages the system via a remote computer. Different injector types were used depending first on the fuel and the engine destination (diesel/bio-diesel, gasoline/alcohol) and the nozzle configurations like single/multi-holes, final duct geometry (k-factor) and orientation (pintle with inward/outward opening, …).

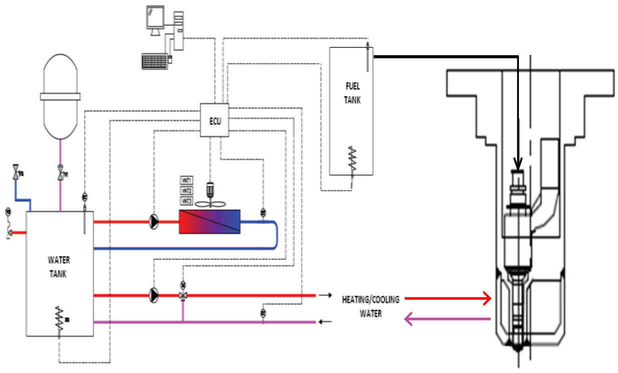

Figure 2: Schematic of the nozzle and fuel temperature governor

The injectors were driven by a homemade Programmable Electronic Control Unit (PECU) reproducing the exciting current profile. Each of them is correlated with a “fuel injection rate” profile permitting to measure the reactivity of the device to the energizing current from the PECU such as the instantaneous amount of fuel delivered through the nozzle.
As an example, Figure 3 reports the solenoid current driving a Gasoline Direct Injection (GDI) electron injector (top) and the corresponding fuel injection rate (bottom) at 15.0 MPa pressure and 1.0 ms duration. The total amount of delivered fuel is integral along with the actual duration and corresponds to 4.19 mg while a delay of 300 μs registers between the start of the command and the first exit of the fuel from the nozzle. The actual duration of the injection is about 1.3 ms. The fuel injection rate was measured by an AVL gauge system working on the Bosch tube principle [11].
The injection happens in a small chamber geared with a piezo-quartz pressure transducer located very close to the nozzle exit. The injection cell is connected to a constant-section long pipeline for absorbing the pressure wave generated by the fuel. It is kept at a constant pressure of 1.0 MPa for avoiding cavitation phenomena [11, 12].
The pressure signal collected in the chamber is proportional to the injection rate through geometrical parameters of the apparatus and the chemical-physical properties of the fluid. The measures were averaged on one hundred shots and restrain the dispersion is less than 2%, and the results compared with that pounded at the Bosch tube discharge by a precision balance [13].

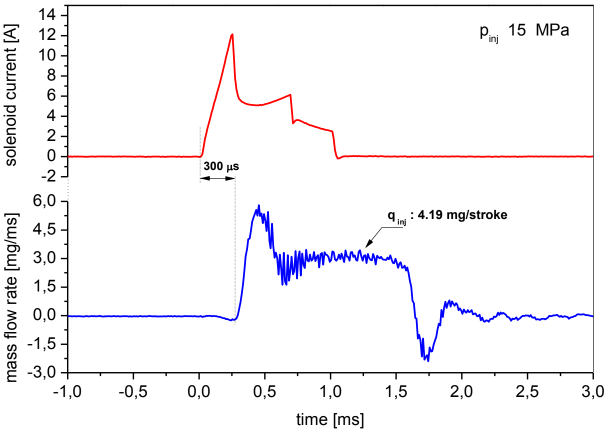

Figure 3: Typical solenoid injector driving current (top) and mass flow rate (bottom)

2-1) Optical Setup

For multiphase fluids, both the liquid and vapor phases contribute to the signature picture. This makes it impossible to definitively distinguishing the vapor phase from the liquid one without an integrative measurement. The author's choice was to investigate the spray by two optical techniques, schlieren, and Mie scattering. The acquisition of the images along the same line-of-sight allows the Mie scattering images to be overlaid onto the schlieren images enabling to mark the phase boundaries.
High-speed Mie scattering imaging was utilized to visualize the liquid phase while the corresponding schlieren one was employed to visualize the vapor phase.
The schlieren setup was realized according to the traditional Z-folded configuration using two 15° off-axis parabolic mirrors (4-inches in diameter, 508 mm parent focal length). The images were acquired using a high-speed C-Mos camera (Photron FASTCAM SA4), at rates up of 45,000 frames per second (fps, image window of 384x192 pixels). The camera was equipped with a 90 mm objective, f 1:2.8, resulting in spatial resolutions up to 4.5 pixel/mm. A sketch of the optical setup is reported in Figure 4.

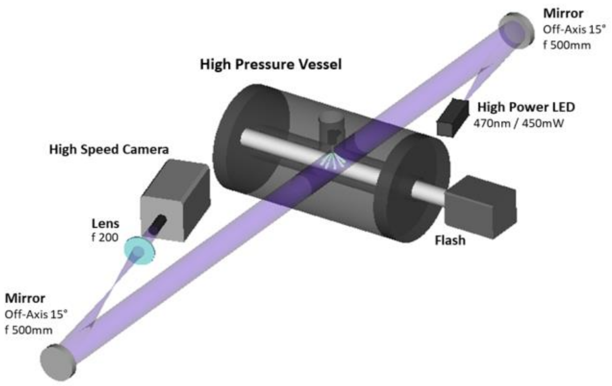

Figure 4: Schematic of optical set-up.

2-2) Image processing

The desired parameters of the spray developments were extracted by a suitable image processing procedure. Contours of the liquid phase were obtained by segmenting the scattering images of the spray using optimal filtering of the image, relied on traditional methods combined with an original threshold procedure based on the weighted cumulative application of the Otsu's method [14]. The segmentation of schlieren images, to get the contours of the spray vapor phase, was obtained by exploiting some traditional filters and operations of the image to strongly enhance the intensity texture due to the vapor density gradients. This approach allows discerning the whole vapor phase of the spray from the background. Subtraction and division [15] of background were carried out for removing noises and so guarantee a homogeneous background. Finally, the gamma (γ = 0.6, stretching image) and the Gauss filters (σ = 1, smoothing) were hands-on to highlight the pictures under process. The binarization, so the boundary, was obtained utilizing the Otsu algorithm [14] applied at the latter image.
Finally, the contour shapes of the spreading fuel for both the liquid (from Mie scattering images) and the vapor phases (from schlieren images) were superimposed to the original image. An in-house algorithm in MATLAB platform was developed to process the images through the main macroscopic parameters characterizing the liquid and vapor phases development: axial and radial penetration versus the time from the start of injection as the maximum elongation in the vertical and horizontal direction, respectively. Further details about the image processing are reported in [16].

3) Results and Discussion

This section is organized in a way to report the before described application on the spray evolutions at engine-like conditions for diesel use, considering the highest thermodynamic conditions of the gas in the combustion chamber and the injection pressures, and for GDI at the condition of the gas type of an Otto-cycle engine. Then, the study of impacting on the heated wall, simulating impingements on the piston wall and cylinder lines will be reported, too.

3-1) Fuel injection rates

Measurements of the fuel injection rate were

made by an AVL meter for a single pulse strategy at 70, 120 and 180 MPa injection pressures and 1.0 ms pulse duration. Each profile is the averaged result for one hundred shots to reduce the noise of the single measure. A single-hole nozzle, axially-disposed, 0.10 mm in diameter was used injecting monocomponent n-heptane fluid. Figure 5 reports the fuel injection rate profiles for the investigated injection pressures. The injected quantities are the integrals of each profile along with the pulse durations.
These measured values have been compared with the weighted fuel collected at the discharge pipe; accordance in a range of 2% has been found. The initial rise times of the signals are perfectly overlapping indicative of the reliability of the injectors. The close time and the stationary phase level increase with the injection pressure for both injectors. Moreover, a delay of 0.34 ms of the injection rate profiles, respect to the start of energizing currents, has been measured due to the hydraulic delay.

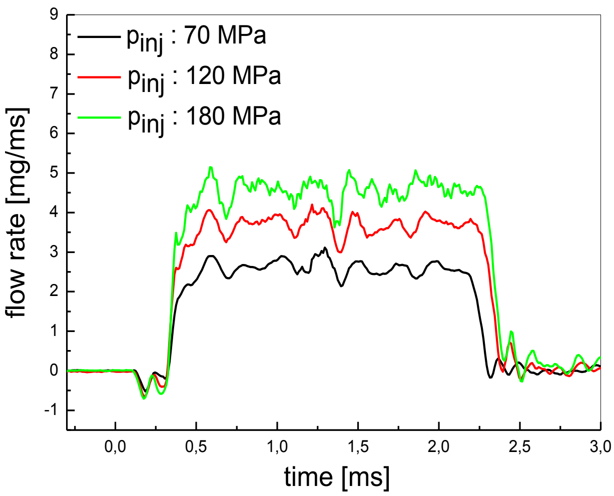

Figure 5: Flow rate profiles at three injection pressures

3-2) Liquid and vapor distribution for an n-heptane spray

These results are referred to as the behavior of a spray produced by, evolving in the vessel at typical conditions of a diesel engine. The activity was a fruitful collaboration between the Istituto Motori (IM) in Italy and the Michigan Technological University (MTU) in Michigan. Before reporting the results, a brief description of the preburn process is hereafter. A flammable preburn mixture of C_2H_2, H_2, O_2, and N_2 is mixed according to the volume fraction of 3.2% C_2H_2, 0.5% H_2, 8.2% O_2, and 88.1% N_2 to obtain inert conditions (0% O_2) at the injection time. The CV is filled with this mixture to 3.39 MPa, which corresponds to a gas density of 23.9 kg/m^3.
The electrical spark is triggered inside the CV to ignite the combustible mixture and the mixing fan starts to generate turbulence to make a homogeneous mixture of combustion products.
Gas temperature (T_g) rises to about 2000 °K. After the combustion event, the CV temperature and pressure gradually decrease undergoing the cool down phase due to the heat transfer to the relatively cold CV walls. Fuel injection is triggered when the desired target temperature (900 °K) is reached during the cooling down process. Note that the initial O_2 in the preburn mixture has been consumed by the combustion of C_2H_2 and H_2 and therefore, the residual O_2 mole fraction is about 0%. At these conditions, the injected spray vaporizes only and doesn't auto-ignite because of the zero oxygen level. Conversely, if the initial percentage of O_2 gas is 23%, a residual fraction of about 15% remains in the vessel and the fuel inject can burn.
The liquid and vapor phase distribution of the sprays captured has been studied under non-reacting conditions spraying in the combustion vessel where the pre-burning of the gas generated high-temperature and high-pressure environment. The early part of the spray shows a solid dark jet, mainly identified as the liquid phase of the emerging spray characterized by a high momentum and density.
It does not appear transparent. The vapor segment length can be determined as differences between the total length of the jet and that of the liquid phase. Figure 6 shows a sequence of images, at different time ASOI, with boundaries of the liquid and vapor phases as emerges from the computer processing. The red and green lines delimit the liquid and vapor area, respectively. At the early time (0.04 ms) only the liquid phase is present. Later, the vapor area increases while the liquid one remains fairly constant.
The liquid, the vapor as well as the combustion pictures for the reacting conditions (15% O_2) are reported in Figure 7. The sequence is just across the starting of the combustion (SOC) phase that starts at the front of the spray and is well recognizable for the high luminosity that saturates the camera.
Chemiluminescence signal becomes visible and indicates the start of diesel fuel auto-ignition.

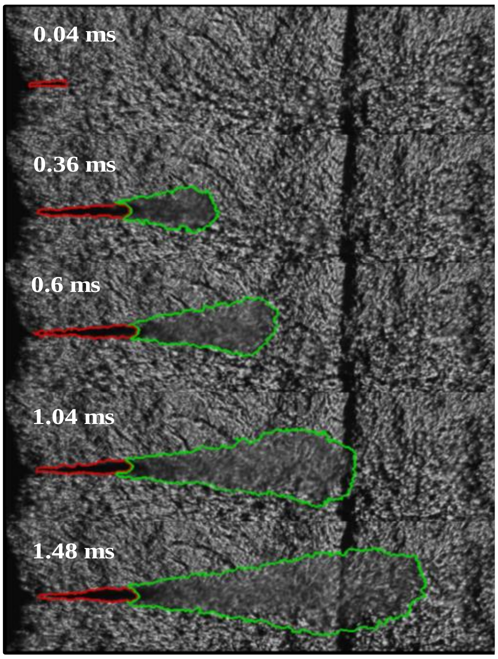

Figure 6: Liquid and vapor envelopes for p_{inj}:70 MPa, T_g:900 K and gas density 23.9 kg/m³

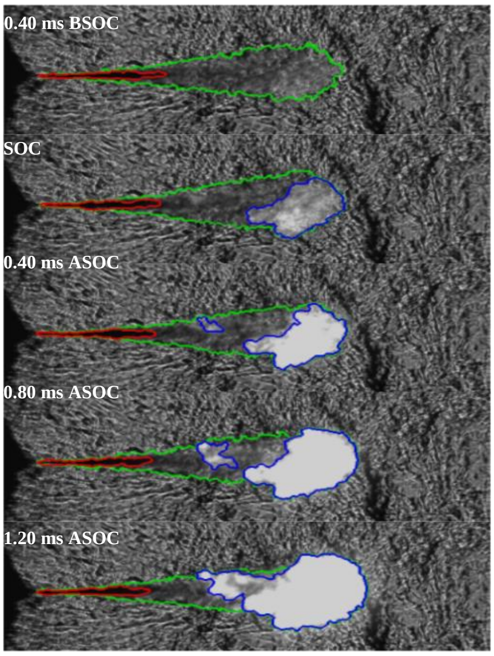

Figure 7: Liquid, vapor, and combustion envelopes for p_{inj}: 70 MPa, T_g: 900 °K and gas density 23.9 kg/m³

The initial stage has a relatively lower chemiluminescence level without saturating the CCD chip of the camera. But with the rapid combustion proceeds, soot begins to form and gets oxidized. The luminosity of soot burning rapidly dominants the image and saturates the CCD. In this figure, the blue contour limits the combustion area diffusing backward the nozzle direction while, as a convention, the green and the red lines delimit the vapor and the liquid phases, respectively.

Finally, Figure 8 reports the tip penetrations of the liquid and the vapor phases for the non-reacting and reacting conditions at the injection pressures of 70, 120 and 180 MPa. Both the liquid and vapor phases overlap in penetrating up to the start of the combustion. Hereafter, the penetrations of the reacting vapor overcome the non-reacting ones due to the increased pressure generated by the combustion while, conversely, the liquid phase collapses because of the temperature increase that fastens the vaporization process.

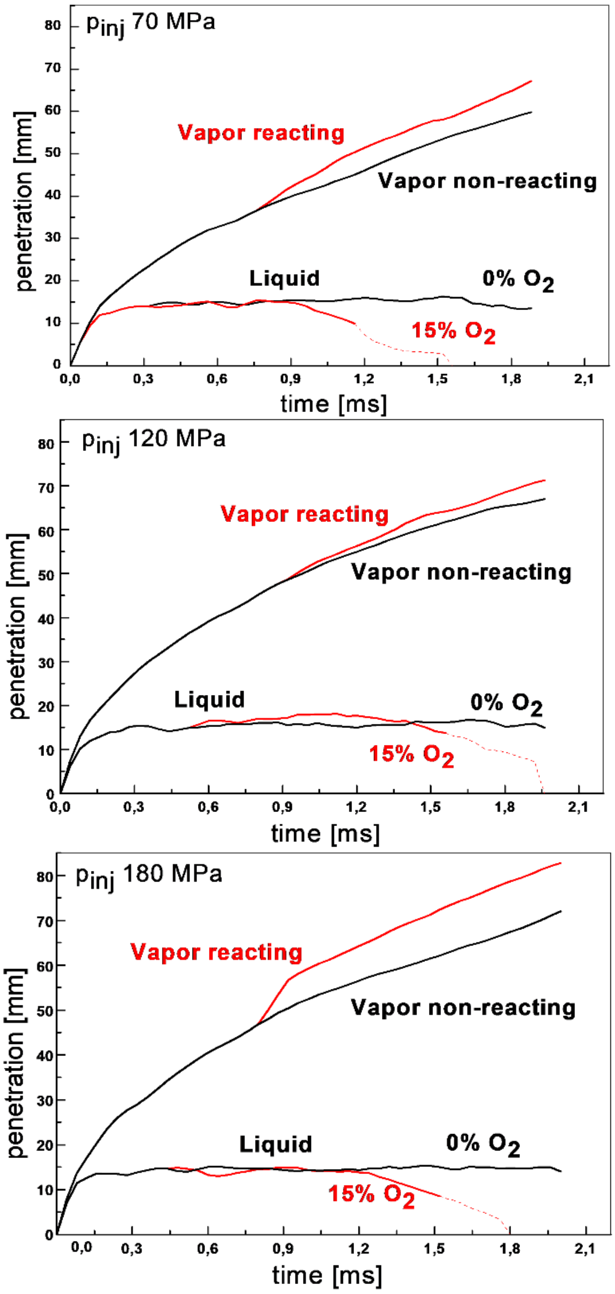

Figure 8: Liquid, non-reacting vapor, and reacting vapor for p_{inj}:70 MPa, T_g:900 K and gas density 23.9 kg/m³

3-3) Gasoline Direct Injection

The use of Gasoline Direct Injection (GDI) continuously increases due to the growing demand for efficiency and power output for i.c. engines. GDI enables stratified and overall lean combustion for a large range of engine operating conditions [5] while permits homogeneous charge for full load requirement. For these systems and with the help of electronic control, the fuel atomization and evaporation could be well controlled and well-atomized sprays are obtained fastening the vaporization process and the mixture preparation. As the main drawback, a high quantity of fuel may impact on the piston head and cylinder liner with HC production and particulate matter, too.

The optical techniques are a very powerful tool for a deep characterization of a GDI device in terms of liquid and vapor fuel distribution evolving in a quiescent volume at engine-like conditions exploring a wide range of injection/ambient conditions and considering the effects of the gas density and temperature, injection pressure and flash-boiling context on the fuel distribution. Sequences of liquid and vapor images of the iso-octane were frozen by Mie-scattering and schlieren techniques on a high-speed C-Mos camera. The reported results are referred to as the use of a non-commercial peculiar injector that was designed and built for the Engine Combustion Network (ECN) [8], and is an eight-hole, circularly disposed on the nozzle and centered with its axis, having cylindrical shape and diameter of 165 m.

3-3-1) Effects of the gas density

The density of the gas in the vessel is the foremost controlling parameter of the fuel spread in the combustion chamber, representing the main impediment to the droplet traveling while gives a strong contribution to the atomization process.

The test conditions were carried out at the fixed gas temperature of 573 °K is the fluid injected at 20.0 MPa and the explored densities of 0.2, 0.5, 1.12, 3.5, and 7.0 kg/m^3. Figure 9 reports schlieren images of the history of the spray evolution as a function of diverse injection timings and gas densities. Some of the sceneries do not realize in the engine (like 0.2 kg/m^3) but they are useful for understanding the thermodynamic behavior of the fluid at that state. The highest densities represent an obstacle to the traveling droplets acting as a brake: the penetrations shorten themselves while the cone angles vary, considering the hollow umbrella morphology of the spray. These behaviors are well evident at the longest time from the SOI when the sprays are completely developed. The effect of the fuel vaporization (573 °K > 372 °K, vaporization of iso-octane) starts from the neighbors of the single plume where particles are smallest in size due to the strongest interaction with the gas while the first column (and partially the second) emphasizes the flash-boiling effects.

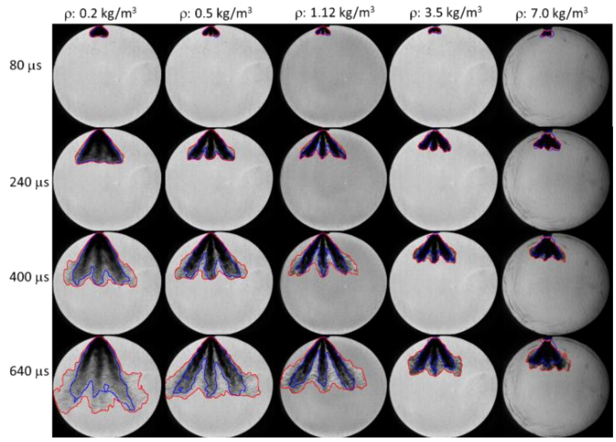

Figure 9: Schlieren spray images for different gas densities; p_{inj}: 20 MPa and T_g: 573 °K

Figure 10 reports the liquid (top) and vapor (bottom) penetrations of the spray for the different back-densities with a well-scaled behavior at increasing of the braking effect produced from the gas.

3-3-2) Effects of the gas temperature

The consequences of the temperature variations of the gas in the vessel (T_g) on the spray spread at the injection pressure of 20.0 MPa while the temperature of the gas was increased at 333, 373, 473, and 573 K were explored.

The influence of the temperature on the spray evolution at the ambient gas density of 1.12 kg/m^3 is reported in Figure 11 where a strip of images, frozen at 640 μs for the liquid phase, is depicted at the top while, at the bottom, a sequence of schlieren frames is reported highlighting the vapor phase.

The consequence of the temperature increase in the liquid part of the spray is well emphasized by the images collected by the Mie-scattering technique (top).

At temperatures of the gas less than the iso-octane vaporization one (372 °K), the plumes are

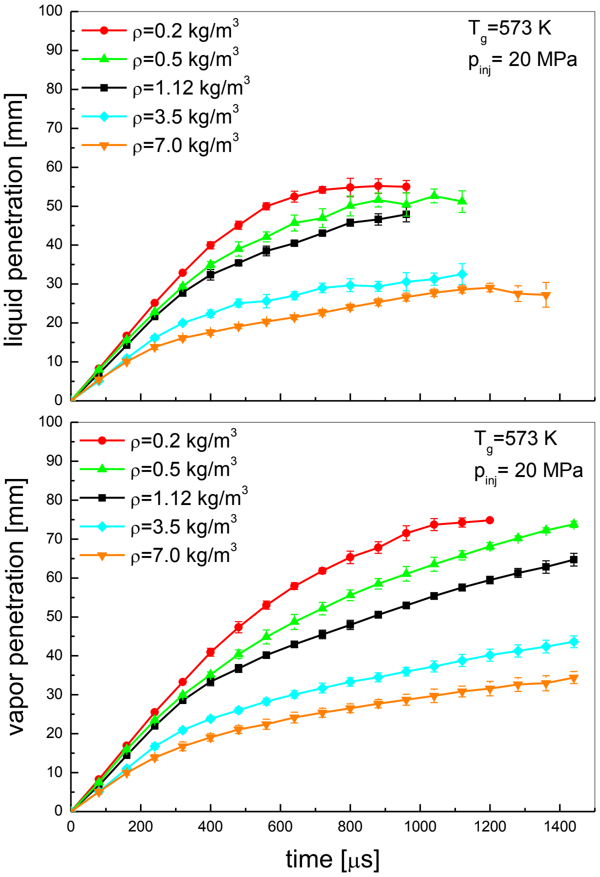

Figure 10: Effect of gas density on liquid (top) and vapor (bottom) penetration; p_{inj}: 20 MPa, T_g: 573 °K.

constituted essentially of a liquid part, the jets are bulky and the longest penetrations are reached. Conversely, the increase of the temperature causes the spray to become skinny and the penetration shorter because of the evaporation process as shown in Figure 11. The frames corresponding to 473 and 573 °K show the position of the vapor phase of iso-octane mainly located on the front and the neighbors of the plumes giving evidence of the slimming and shortening of the liquid phase.

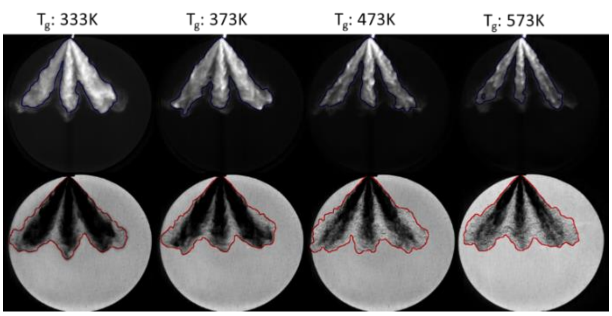

Figure 11: Mie-scattering (top) and schlieren (bottom) spray images as a function of the ambient temperature; p_{inj}: 20 MPa, ρ: 1.12 kg/m³, t_{inj}: 640 μs.

3-3-3) Flash-boiling conditions

The flash boiling is a thermodynamic instability of a liquid jet operating under superheated conditions. As the ambient pressure goes below the fuel saturation value, it reaches a metastable state and a rapid boiling of the liquid could occur [17- 19]. This condition could occur injecting into sub-atmospheric pressures that typically happens at the full-load condition and early-time injection for GDI engines. Significant phenomena are associated with this wide variety of thermo-dynamic conditions: the most important and highly influencing the atomization process of the fuel is the "flash-boiling".

In Figure 12, images of sprays, injected at 20.0 MPa of pressure and frozen at 640 μs from the SOI, are reported for the gas temperatures of 333, 373, 473, and 573 K, and realizing gas densities of 0.2, 0.5, and 1.12 kg/m³ being constant the fuel (T_f) and the nozzle temperature (T_i) at 363 K. These settings configure the sub-atmospheric conditions in the vessel for the "flash-boiling" effect [16].

Referring to the 1.12 kg/m³ density (atmospheric), the structures of completely developed spray in sub-atmospheric conditions appear remarkable. At the temperature of 333 K (less than iso-octane boiling point), the silhouette at 0.5 kg/m³ sketches a slight umbrella angle reduction with a partial overlapping and an initial closure of the plumes close to the nozzle.

This effect is hugely emphasized at 0.2 kg/m³ where the eight jets collapse completely in a unique mushroom-like figure with the fluid occupying the empty volume inside the spray. The 0.2 kg/m³ condition realizes a ratio *pa/ps* less than 1 that design the flash-boiling condition, being *pa* the ambient pressure in the vessel and *ps* the saturation pressure of the liquid.

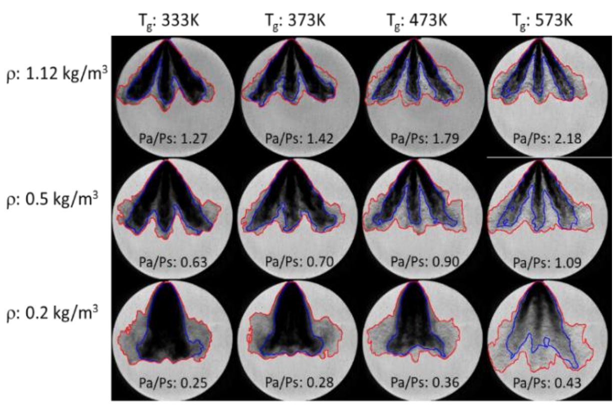

Figure 12: Schlieren spray images for different ambient temperatures and gas densities; p_{inj}: 20 MPa, t_{inj}: 640 μs

The curves at the top-left side of Figure 13 depict the axial penetration of the liquid fuel for the 0.2, 0.5, and 1.12 kg/m³ gas densities at the ambient temperature of 333 K and pressure of 20.0 MPa.
The profiles show a regular growth vs time and a well-scaled behavior concerning the gas densities. The penetrations decrease with the increase of the ambient pressure due to the growth of the drag force effect.
The graphs overlap up to 320 µs indicating a negligible initial effect of the density and that the controlling parameter results in the early momentum of the fuel bulk. Later, the lower is the density and the higher are the penetration lengths.
The motivation is to be attributed to the effects of flashing that produce a collapse of the spray, increasing the penetration and reducing the cone-angle. These results are confirmed in the cone-angle graphs, reported on the top-right part of Figure 13.
The penetrations of the vapor portions (bottom-left of Figure 14) show analog behaviors of the liquid ones. The initial overlapping keeps up to 240 µs, later the trend gives back the highest penetrations for the lowest densities. The cone angles, reported at the bottom-right side of Figure 13, depict a constant value of 77.5° for the 1.12 kg/m³ setting, while the 0.5 kg/m³ condition starts from 79.8° and decreases up to 74.8°. Last, the flashing (0.2 kg/m³) reduces the angle to 48.8° with a slightly decreasing tendency up to 46.1°.

3-3-4) Fuel distribution for spray impacting on a heated wall

The impingement of liquid fuel on combustion chamber walls is one of the major drawbacks in GDI engines producing an increase in HC and particulate matter emissions. The impact is enhanced by the high pressures of injection and the downsizing trend in powertrains making shorter the nozzle-piston head distance.

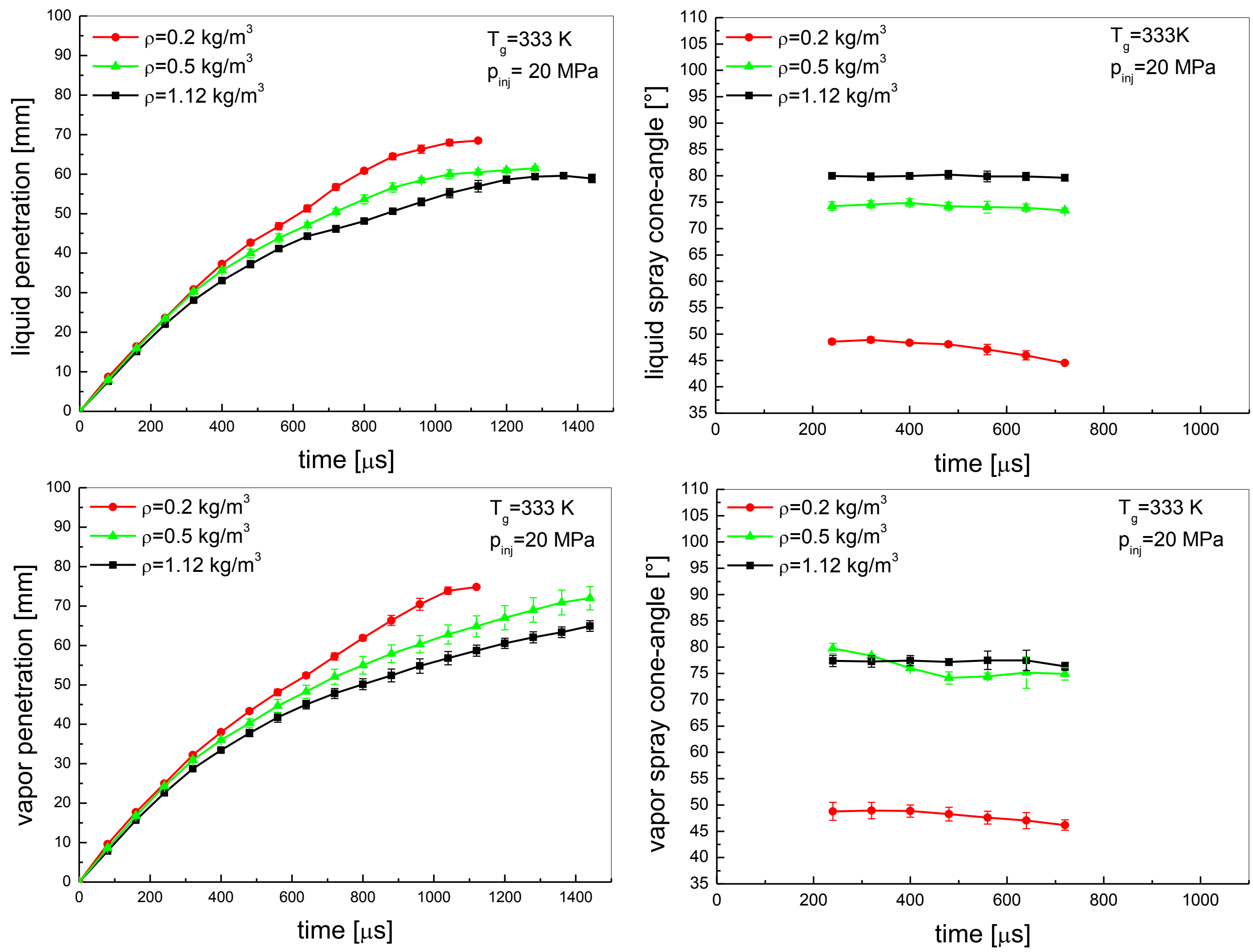

Figure 13: Top: liquid penetration and cone-angle as a function of the gas density; bottom: vapor penetration (left) and cone-angle (right) as a function of the gas density; Tg: 333 K, p_{inj}: 20 MPa

The surface temperature of the wall is identified as an important parameter affecting the outcome of the fuel after impact. Hence, the necessity of a detailed understanding of the spray-wall impingement processes and their effects on fuel distribution. The tests were carried out allocating an 80 mm in diameter aluminum flat plate 22.5 mm downstream to the injector tip and placed orthogonally to the injector axis. The wall temperature [T_w] was varied from room to 573 °K by an electric resistance and monitored in temperature by a J-type thermocouple. The ambient temperature [T_g] inside the vessel was kept constant at the same wall temperatures.

The aim was to understand the interaction between the injected iso-octane and the wall under engine-like conditions observing, by cycle-resolved simultaneous Mie scattering and schlieren images, both the liquid and the vapor phases as the surface temperature varied from 293 to 573 K in N_2 environment at 1.12 kg/m^3. The eight-hole GDI injector, from ECN Net-work, was used. The surveyed parameters were, both for the liquid and vapor phases, the extensions of the width and thickness, as a function of the time, of the fuel figure after the impact vs the injection pressure and the temperature of the plate. These parameters are represented in Figure 14.

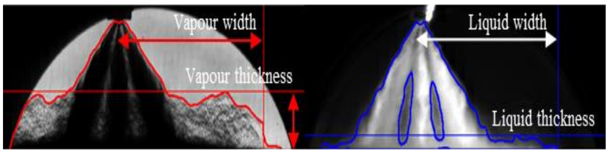

Figure 14: Liquid and vapor outlines with width and thickness definitions on schlieren (left) and Mie-scattering (right) images

Before the impingement, the spray develops and atomizes as a free spray. After the impact, reflected droplets become smaller compared to incident ones, which means these are mainly derived from splash and secondary breakup [16]. The pictures at successive instants depict a mixture of vapor and liquid phases of iso-octane flushing along the wall and rebounding on it. The fuel develops on the wall in regular and symmetrical mode on both sides concerning the injector axis. Vortexes are formed at the jet periphery due to the interaction with the wall and the gas.

The slipping/rebounding fluid shows a double structure: denser and impenetrable to the schlieren light beam close to the wall, indicative of a predominance of the dense liquid phase, lighter and almost transparent upper the plate, symptomatic of vapor generated by the heat exchange with the wall.

Figure 15 reports an impacting spray sequence at different wall temperatures (from 293 to 573 °K) from Mie scattering (top) and schlieren (bottom) optical techniques. The imagines refer to the time step of 480 s after the impact and the injection pressure is 20.0 MPa.

For each column, the effects of the wall temperature can be evaluated on the liquid phase from Mie-scattering images and vapor from schlieren ones. The increment of the wall temperature affects both the liquid, with much-dispersed droplets, and vapor phases. It determines a shift of the impact regime from deposition towards rebound or thermal break-up, thus leading to enhanced vaporization.

Looking at the schlieren spray images in Figure 15, the mixed area, over-hanging the liquid portion (dark part immediately on the wall), includes ligaments, droplets more or less finely atomized and vapor phase. The growth of this area appears evident when the temperature increases; the higher is the temperature of the wall the stronger the characteristic vortexes of the vapor phase appear.

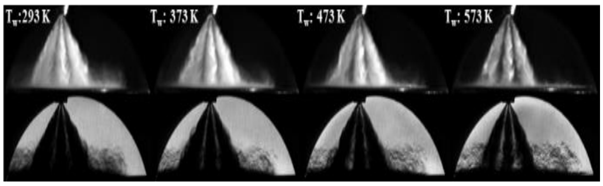

Figure 15: Impacting spray images at 480 s after the spray impact for different temperatures of the wall

The fuel vaporization is encouraged mainly by two factors: the impact that contributes to the droplets breaking, facilitating the evaporation process, and the heat exchange with the wall giving a contribution to the latent heat of vaporization and determining secondary evaporation. As a consequence of the vaporization process, a strong reduction of the liquid thickness comes out by looking at the Mie-scattering images when increasing the wall temperature from 293 value to 573 °K.

Figure 16 depicts at the top of the liquid and vapor width behavior vs. the wall temperature from 293 to 573 °K at an injection pressure of 20.0 MPa. Both liquid and vapor profiles show a

quasi-linear grow vs time for all the investigated temperatures. The increment of the temperature from 293 to 373 °K doesn't produce any detectable effect on liquid and vapor slipping; in fact, the curves (black and red respectively) overlap for all the entire injection duration. For temperatures higher than the vaporization value of the iso-octane (372 °K), the curves show a well-scaled trend of both liquid and vapor length concerning the wall temperature, higher is the temperature and faster the fuel slipping results. The curves reported at the bottom of Figure 16 depict the behavior of the liquid and vapor thickness rebounding from the surface as a function of its temperature at the injection pressure of 20.0 MPa. The liquid thickness shows an inverse trend concerning the wall temperature with the strongest rebound at room value (black line).
At the lowest temperatures of the wall, the thickness evolves in time tending to a maximum: around 700 μs (about 7 mm) at 293 °K and decreasing around 400 μs (about 4 mm) at 373 °K. Vice-versa, at values of 473 and 573 °K the trend is still of increasing versus the time from the impact only up to 200 μs with a quick tendency to saturate towards a stable value, around 2 mm, indicating a faster fuel evaporation.

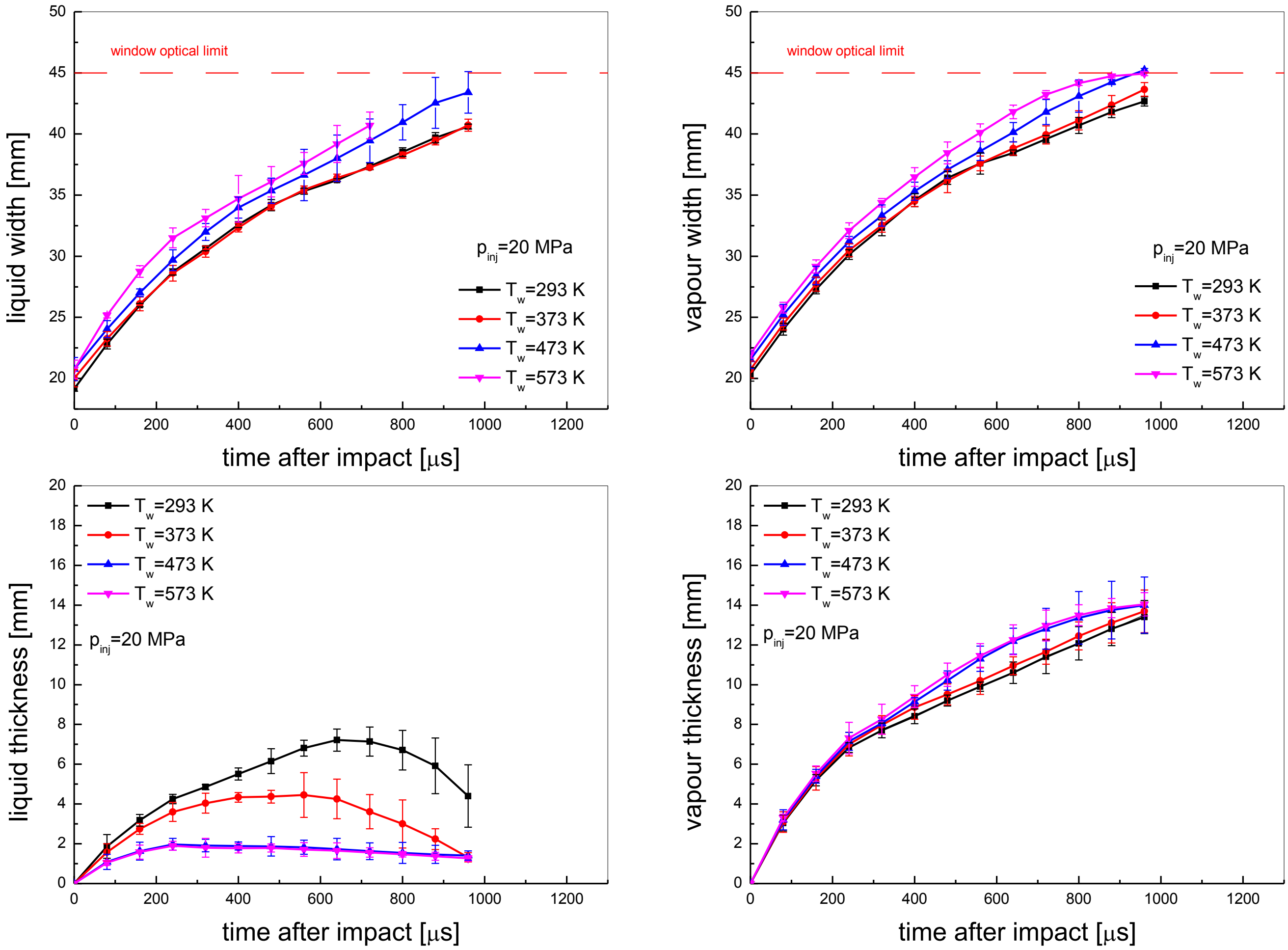

Figure 16: Liquid and vapor width (top) and thickness (bottom) at different wall temperatures

4) Conclusions

A review of optical techniques applied to the fuel spread in internal combustion engines was reported in this paper for diverse ambient conditions, different fuels, and differentiate injection systems. Engine-like thermodynamic conditions were realized in a quiescent vessel, optically accessible, permitting free evolving spray inside in non-evaporating and evaporating conditions such as impacts on heated wall simulating the piston head or cylinder lines.

Direct injection of both gasoline and diesel fuels were simulated with liquid and vapor phases depending on the ambient conditions. Non-interfering optical techniques were adopted: Mie-scattering for the liquid and shadowgraph/schlieren for the vapor phases in a cycle-resolved sequence of images for the evolving jets, then processed for extracting the required parameters.

The liquid, vapor, and combustion phases were highlighted for an n-heptane fluid in diesel-like conditions using a pre-burn procedure for reaching thermodynamic conditions of a diesel engine. The technique was successful for catching peculiar parameters as penetrations, cone-angles such as lift-off length for a single-hole injection device.

Iso-octane has been injected by GDI systems, adopting the eight-hole spray G from the ECN Network. A wide set of conditions like injection pressure, back-densities, gas temperatures permitted to characterize the free evolving spray and the liquid and vapor phases were measured in terms of penetrations and cone-angles by the acquired images. The effects of the gas density in the vessel, its temperature such as the injection pressure on the liquid diffusion were evaluated. Important effects related to the flash-boiling conditions, occurring for superheated conditions of the fuel at peculiar gas densities and temperature were depicted.

Finally, the condition of the impact of the fuel a heated wall was highlighted where iso-octane impinged on aluminum plate simulating the piston head or the cylinder line. A wide range of plate temperatures such as injection pressure were investigated with the measurements of droplet slipping and rebounding on the wall named width and thickness. The adopted techniques permitted a detailed description of the liquid and vapor phases and their dependence on the ambient conditions.

List of Symbols

ASOI	After Start Of Injection
CCD	Charge-Coupled Device
CFD	Computational Fluid Dynamics
CV	Combustion Vessel
DI	Direct Ignition
ECN	Engine Combustion Network
fps	Frames per second
GDI	Gasoline Direct Injection
HC	Hydrocarbons
i.c.	Internal combustion
LED	Light Emitting Diode
PECU	Programmable Electronic Control Unit
PFI	Port Fuel Injection
p_a	Ambient pressure
p_s	Saturation pressure of the liquid
p_{inj}	Injection Pressure
q_{inj}	Amount of injected fuel
ρ	Ambient gas density
SOC	Start Of Combustion
T_f	Fuel temperature
T_g	Ambient temperature
t_{inj}	Injection timing
T_w	Wall temperature
T_i	Nozzle temperature
TTL	Transistor Transistor Logic

References

[1] Mahr, B., "Future and Potential of Diesel Injection Systems," THIESEL 2002 Conference on Thermo- and Fluid-Dynamic Processes in Diesel Engines, 2002

[2] Brusiani, F., Bianchi, G., Falfari, S., Onorati, A. et al., "Influence of Cylindrical, k, and ks Diesel Nozzle Shape on the Injector Internal Flow Field and the Emerging Spray Characteristics," SAE Technical Paper 2014-01-1428, 2014, DOI:10.4271/2014-01-1428

[3] Kale, R., and Banerjee, R. 2019a. Experimental investigation on GDI spray behavior of isooctane and alcohols at elevated pressure and temperature conditions. Fuel, 236, 1–12. ISSN 0016-2361. DOI:10.1016/j.fuel.2018.08.153

[4] Parrish, S. 2014. Evaluation of liquid and vapor penetration of sprays from a multi-hole gasoline fuel injector operating under engine-like conditions. SAE Int. J. Engines, 7(2), 1017–1033. DOI: 10.4271/2014-01-1409

[5] Zhao, F., Lai, M.C., and Harrington, D.L. 1999. Automotive spark-ignited direct-injection gasoline engines. Prog. Energy Combust. Sci.,

25(5), 437–562. DOI: 10.1016/S0360-1285(99)00004-0

[6] Köpple, F., Jochmann, P., Kufferath, A., and Bargende, M. 2013. Investigation of the parameters influencing the spray-wall interaction in a GDI engine -prerequisite for the prediction of particulate emissions by numerical simulation. SAE Int. J. Engines, 6(2), 911–925. DOI: 10.4271/2013-01-1089

[7] Shim, Y.S., Choi, G.M., and Kim, D.J. 2009. Numerical and experimental study on effect of wall geometry on wall impingement process of hollow cone fuel spray under various ambient conditions. Int. J. Multiphas. Flow, 35, 885–895. DOI: 10.1016/j.ijmultiphaseflow.2009.06.004

[8] Engine Combustion Network data archive http://sandia.gov/ECN/

[9] Abraham, J., Pickett L.M., "Computed and Measured Fuel Vapor Distribution in a Diesel Spray", Atomization and Sprays 20:241-250, 2010

[10] Pastor, J., Payri, R., Garcia-Oliver, J., and Nerva, J., "Schlieren Measurements of the ECN-Spray A Penetration under Inert and Reacting Conditions," SAE Technical Paper 2012-01-0456, 2012, DOI:10.4271/2012-01-0456

[11] Bosch, W., "The Fuel Rate Indicator: A New Measuring Instrument For Display of the Characteristics of Individual Injection," SAE Technical Paper 660749, 1966, DOI:10.4271/660749

[12] Wallace, I., "Injection Rate Gauge: Pass Off Information and User Instructions", Fuel & Engine Management Systems, Graz - December 2002.

[13] Allocca, L., Alfuso, S., Corcione, F. E., "Assessment of Dynamic Performances of Diesel Solenoid Injectors for a Multiple Injection Common Rail System," SAE Technical Paper 2003-01-21

[14] Otsu, N., "A Threshold Selection Method from Gray-Level Histograms," IEEE Trans. Systems, Man and Cybernetics 9(1):62-66, 1979

[15] Russ, J.C., The Image Processing Handbook Second Edition (CRC Press, 1995). ISBN:0-8493-5216-1.

[16] Montanaro, A., Allocca, L., Beatrice, C., and Ianniello, R., "Outwardly Opening Hollow-Cone Diesel Spray Characterization under Different Ambient Conditions," SAE Technical Paper 2018-01-1694, 2018, DOI: 10.4271/2018-01-1694

[17] Allocca, L., Montanaro, A., Di Gioia, R., and Bonandrini, G., "Spray Characterization of a Single-Hole Gasoline Injector under Flash Boiling Conditions," SAE Technical Paper 2014- 32-0041, 2014, DOI: 10.4271/2014-32-0041

[18] Huang, Y., Huang, S., Huang, R., and Hong, G., "Spray and Evaporation Characteristics of Ethanol and Gasoline Direct Injection in Non-evaporating, Transitional flash boiling and Flash-boiling Conditions," Energy Conversion and Management 108:68-77, 2016

[19] Zeng, W., Xu, M., Zhang, G., Zhang, Y. et al., "Atomization and Vaporization for Flash-boiling Multi-Hole Sprays with Alcohol Fuels," Fuel 95:287-297, 2012

[20] Montanaro, A., Allocca, L., and Lazzaro, M., "Iso-Octane Spray from a GDI Multi-Hole Injector under Non- and Flash Boiling Conditions," SAE Technical Paper 2017-01-2319, 2017, DOI: 10.4271/2017-01-23

فصلنامهٔ علمی- پژوهشی تحقیقات موتور

تارنمای فصلنامه: www.engineresearch.ir

بررسی تجربی تهیه مخلوط سوخت در موتور احتراق داخلی با استفاده از روش‌های نوری

لویجی آلوکا[۱]*، آلساندرو مونتانارو[۲]

[۱] محقق ارشد مؤسسه تحقیقات موتور CNR ایتالیا، ناپولی، ایتالیا، l.allocca@im.cnr.it

[۲] محقق مؤسسه تحقیقات موتور CNR ایتالیا، ناپولی، ایتالیا، a.montanaro@im.cnr.it

* نویسندهٔ مسئول

چکیده

اهمیت تهیه مخلوط مناسب در موتور احتراق داخلی بر هیچکس پوشیده نیست و ارزش تهیه مخلوط در کارکرد درست چرخه ترمودینامیکی برای همه محققین مشخص است. مدت کوتاه میان پاشش سوخت و شروع احتراق برای تهیه بهترین مخلوط و آزاد شدن بهینه انرژی و تولید آلاینده، بسیار مهم است. قوانین سخت‌گیرانه مربوط به انتشار گازهای گلخانه‌ای سبب شده است که محققین موتور به سمت استفاده از سامانه‌های فشار قوی و تزریق مستقیم برای ایجاد بهترین مخلوط سوخت حرکت کنند. شایان ذکر است که کوچک‌سازی موتور منجر به افزایش تأثیر سوخت بر روی هیدروکربن نسوخته و ذرات دوده در خروجی موتور می‌شود. دانش جامعی از سوخت تزریق شده ، پخش شدن آن در محفظه با شکست های اولیه و ثانویه، تبخیر، اختلاط با هوا و احتراق دیدگاه‌های کاملی به محققین داده و در طراحی معماری جدید موتورها کمک شایانی خواهد نمود. روش‌های نوری در توصیف این فرایندها بسیار قدرتمند بوده و در عین حال تداخلی در فرایندهای موتور ندارند. روش‌های تصویربرداری و طیف سنجی به ما اجازه می‌دهد تا تحولات فیزیکی و شیمیایی سوخت در هنگام تهیه مخلوط را بررسی کرده و تولید گونه‌های اولیه و فرعی را دنبال کنیم. در عین حال مکان‌های بالقوه تولید آلاینده در روش‌های نوری به خوبی شناسایی می‌شود. شایان ذکر است که با توسعه این روش در تهیه مخلوط، مجموعه‌ای از داده‌ها برای شروع و نگاشت کدهای عددی آماده می‌شود. در پژوهش حاضر، روش‌های نوری برای به تصویر کشیدن انتشار سوخت در یک محفظه حجم ثابت با شرایط شبیه به موتور، به منظور شبیه‌سازی تزریق مستقیم سوخت در موتور ارایه شده است.

اطلاعات مقاله

تاریخچهٔ مقاله:
دریافت: ۱۶ آبان ۱۳۹۸
پذیرش: ۲۹ بهمن ۱۳۹۸

کلیدواژه‌ها:
موتور احتراق داخلی
احتراق
عیب‌یابی با روش نوری
تزریق مستقیم بنزین
سوخت مایع/ بخار